29th International Cosmic Ray Conference Pune (2005) **10**, 367-376

Acceleration and propagation in the heliosphere

S.W. Kahler[a], K. Kecskeméty[b] and P. Király[b]
(a) Air Force Research Laboratory, Space Vehicles Directorate, Hanscom AFB, MA 01731, USA
(b) KFKI Research Institute for Particle and Nuclear Physics, H-1525 Budapest P.O.B. 49, Hungary
Presenter: S. Kahler (stephen.kahler@hanscom.af.mil)

Heliospheric energetic particles represent a mixture of populations. Sites of original energization of those particles range from solar flares through coronal and interplanetary shocks to distant heliospheric and even galactic sources. Although increasingly sophisticated methods of measuring their energy spectra, composition, charge state, temporal variation and anisotropy help in distinguishing those populations, most studies on particle acceleration and propagation are based on measurements that cannot make such fine distinctions. The lack of clear-cut separation of populations is also reflected in the somewhat ambiguous classification of SH papers in ICRCs. "Solar emissions" and "Galactic cosmic rays in the heliosphere" appear reasonably well separated topics (although Galactic and Anomalous CR could be more appropriate, and space weather as part of the galactic CR topic could be questioned). Acceleration and propagation issues, however, can be only rather artificially separated from the above two. As it happened during this conference, the pre-assigned rapporteur for the "Acceleration and propagation" topic was unable to participate, and the other two rapporteurs for SH topics kindly agreed to report on most papers in the borderline range. Thus we report here only on a relatively small number of papers that could be classified into three general topics: a) Shocks and solar energetic particles; b) Solar energetic particle propagation; c) Radiation environment at Mars.

1. Introduction

The energization of solar energetic particles (SEPs) is mostly a fairly direct consequence of violent solar processes, even when the acceleration occurs beyond the close vicinity of the Sun. Possible acceleration mechanisms include, to mention a few, magnetic reconnection, resonant stochastic acceleration, and diffusive shock acceleration. Shock-related phenomena are usually considered to be responsible for the bulk of the acceleration, and also contribute to the production of seed particles, and modify the propagation of the particles after the acceleration phase. Most of the contributions to be discussed in this rapporteur talk are in some way related to shocks. In addition to the general problems of shock effects in particle acceleration and propagation, a more specific problem of relevance for future Mars missions will also be highlighted.

The distribution of the 23 papers presented according to SH2 classification is as follows:

2.1 Interplanetary transport of energetic solar particles	13 papers
2.2 Propagating interaction regions and shocks	3 papers
2.3 Corotating interaction regions and shocks	2 papers
2.4 Merged interaction regions	0 papers
2.5 General acceleration and transport phenomena	5 papers
2.7 New experiments and instrumentation	0 papers

The disproprtionate distribution of the numbers of contributions both among the three main SH topics and among SH2 subtopics appears to justify a re-thinking of classification schemes.

2. Shocks and SEPs

2.1. Background

The relation between the shock and the spectrum and composition of SEPs has many unknowns. The shock strength, i.e. the compression ratio and the angle between the shock and magnetic field are thought to be vitally important; it is still debated if quasi-perpendicular or quasi-parallel shocks are more effective. Turbulent waves provide scattering, the scattering of particles on self-generated waves results in a non-linear coupling between particles and fields. The seed particles are not yet identified (solar wind vs. pre-accelerated SEPs, nonthermal populations), the role of magnetic field wandering through the shock front is still to be explored.

Currently, the most widely accepted approach is that protons, which are the most abundant species and control the dynamics, generate Alfvén wave spectra, which interact with other charged particles of different charge states and rigidities. This provides the confinement of particles near the shock, which is required for the acceleration. Escape of SEPs from the wave front is rigidity dependent ($R \sim mv/q$). The escaping particles propagate according to the Boltzmann equation. For the simplest spherical case, the phase space distribution function, $f(r,p,t)$ in terms of position, r, momentum, p, and time, t, is given by:

$$\frac{\partial f}{\partial t} = \frac{1}{r^2}\left(\frac{\partial}{\partial r}\kappa_{rr} r^2 \frac{\partial f}{\partial r}\right) - V\frac{\partial f}{\partial r} + \frac{2V}{3r} p \frac{\partial f}{\partial p} + q$$

The first three terms on the right hand side describe diffusion along the magnetic field, convection by the radial solar wind at a speed, V, adiabatic deceleration in the expanding wind, while q accounts for sources (seed population) and/or sinks due to any additional loss process. Particle drifts and cross-field diffusion are neglected here. The equation can easily be rewritten to allow non-spherical geometry or non-uniform solar wind. The inclusion of cross-field diffusion would be desirable, but it would require a fully 3-D treatment. Beside the above robust diffusion equation, another, more sophisticated and computationally more demanding approach assumes field-aligned propagation but retains the full pitch-angle distribution (see Ruffolo 1995, Ng et al. 2003, Tylka 2001 [1]).

Diagnostic tools include in situ SEP charge states, isotopic and elemental abundances, time variations, energy spectra, anisotropies, as well as in situ ambient solar wind particle and magnetic field and wave characteristics.

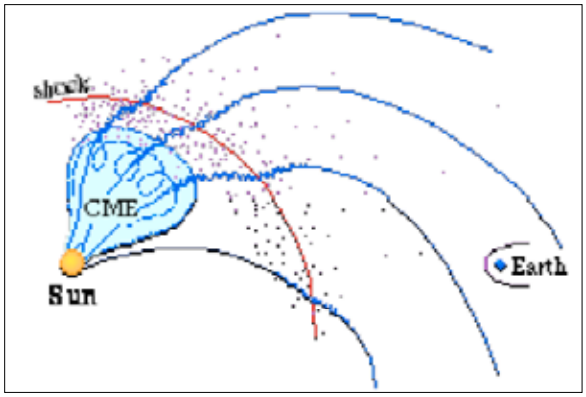

Figure 1. Schematic diagram of the process which creates solar energetic particles (adapted from Lee [2]). A coronal mass ejection drives an interplanetary shock where the SEPs are accelerated

In the shock acceleration process self-generated waves keep SEPs confined near the shock, facilitating efficient acceleration, as discussed by Lee [2]. For other possible models from the SH1 sessions of the present Conference we refer to the rapporteur paper of Ryan [3].

2.2. Shock/SEP association at 1 AU

Questions of shock/SEP associations in different energy intervals were discussed in two of the SH2 contributions.

Cohen *et al.* [4] studied the responses of >10 MeV proton intensities at 1 AU to passing interplanetary shocks for a variety of excess speeds (horizontal axis in Figure 2) and angles between the shock normals and the magnetic fields (vertical axis). Symbol sizes indicate the factors by which intensities increased after the passage of a shock. The excess speed (i.e., the shock speed over and above the SW speed) does appear to us to provide at least a lower threshold (no large intensity increases below excess speeds of 350 km/s), but otherwise the authors find no obvious ordering of intensity increases by either speed or shock angle. The lack of dependence on these parameters is surprising and raises questions for theories of shock acceleration. In addition, the unexpected small fraction of events with substantial intensity increases (only 38 of 354 events) shows that most interplanetary shocks are not accelerationg protons to energies > 10 MeV.

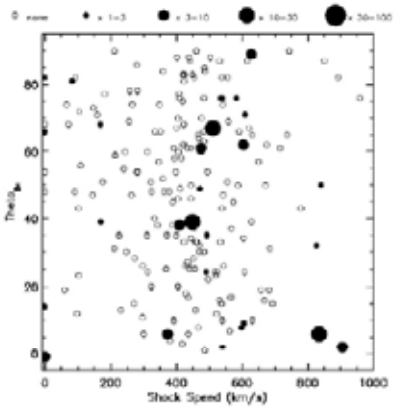

Figure 2. Proton intensity increases measured by ACE/SIS for 354 shocks of measured excess speeds and shock angles. Symbol sizes indicate the factors by which intensity increased at shock passage. Note that only 38 of the shocks caused definite intensity increases, while in 19 cases the intensity either decreased or the decay profile was modified.

Timofeev and Filippov [5] studied particle acceleration by shocks, at high (GeV) energies, during the October – November 2003 events, based on 5-minute data of neutron monitors. Two solar active regions produced three large energetic particle increases and several Forbush decreases during a period of about two weeks. Of particular interest was the GeV energetic particle increase on 28 October (Figure 3) that Timofeev and Filippov attributed to a strong converging shock pair arriving at Earth on 26 and 28 October with speeds of 1100 and 1800 km/s, respectively. Although such converging shock pair acceleration scenarios have already been observed earlier (e.g. in the August 1972 and October 1981 events), this GeV SEP increase is generally attributed to the fast (> 2400 km/s) CME on 28 October associated with the X17 flare at S20 E02 in AR 10486.

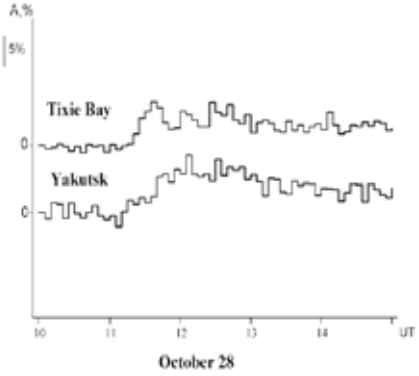

Figure 3. Intensity increases at the Yakutsk and Tixie Bay Neutron Monitors due to the appearance of GeV solar particles on 28 October, 2003.

2.3. Observational and theoretical aspects of some shock/SEP features

Cohen *et al*. [6] discussed extensive observational material related to the powerful late October to early November 2003 solar flare and CME events. ACE/ULEIS and /SIS data were used over more than 3 decades of energy (<0.1 MeV/nucleon to 100 MeV/nucleon) and for elements ranging from C to Fe. At energies above ~10 MeV/nucleon, 5 events were readily identified in the oxygen intensity time profiles. The events differed both in intensity and in spectral shape. Although energy spectra are fairly smooth, it is clear that spectral steepening occurs at different energies in the five events (Figure 4).

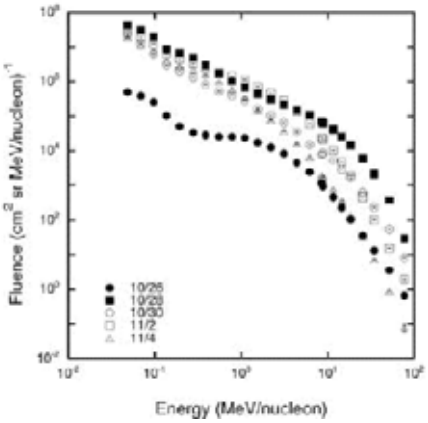

Figure 4. Oxygen fluence spectra for the five late October to early November 2003 events.

Spectral break energies were found to be rigidity-dependent (rather than energy or energy/nucleon dependent) effects in the shock acceleration and transport processes. Spectral steepening can be attributed to rigidity-dependent escape from the shock. From the scalings of spectral breaks for two different elements the inferred wave spectra in the shock regions are considerably flatter than the Kolmogorov spectra characteristic for general interplanetary turbulence. This conclusion is consistent with the dominant role of streaming energetic protons in generating the bulk of the turbulence in the shock region.

Theoretical aspects of interplanetary shock acceleration were discussed by Berezhko and Taneev [7] and by Channok *et al.* [8].

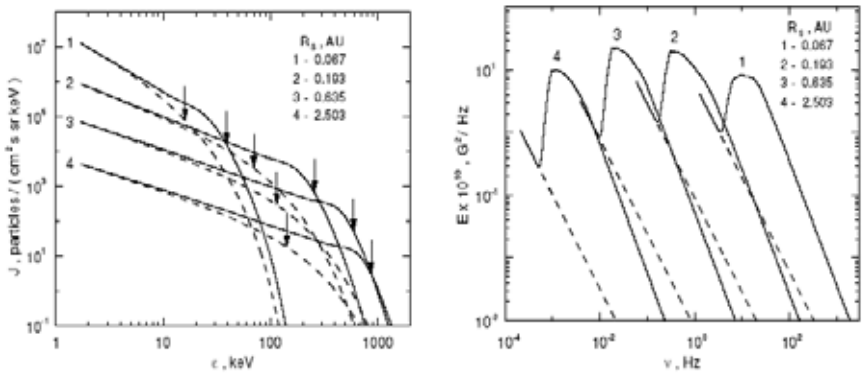

Figure 5. Left: The intensity of accelerated protons at the shock front for four subsequent time moments as presented by Berezhko and Taneev [7]. Solid (dashed) lines correspond to the quasilinear (linear) approach. Arrows indicate the proton maximum energy**.** Right: The spectra of Alfvén waves at the shock front for the same four time moments as on the left-hand side. Solid (dashed) lines correspond to the quasilinear (linear) approach.

In the first paper, a self-consistent theory of ion diffusive shock acceleration and the associated generation of Alfvén waves was presented. The wave intensity satisfies a wave kinetic equation and the ion distribution function satisfies the diffusive transport equation. The authors apply a rate of recently proposed wave generation efficiency (Gordon et al., [9]) that is a factor of 8/3 more effective than the one used previously. These quasilinear non-stationary equations are then solved numerically for a given speed of the shock, traveling through the inner heliosphere. Another new development is that Berezhko and Taneev introduce a loss term to account for sideway escape of particles from the acceleration region due to perpendicular diffusion. Efficient Alfvén wave generation leads to a considerable decrease of particle diffusion coefficient that in turn provides more rapid particle acceleration. Therefore the maximum energy of accelerated protons considerably exceeds its value calculated in the linear approach. Energetic particle spectra and self-consistent Alfvén wave spectra are shown in Figure 5. At early times ($R < 0.3$ AU) the cutoffs of the energy spectra are determined mainly by the acceleration times, while at late time the effect of the shock geometry becomes predominant.

In the Channok *et al*. paper [8] finite-time acceleration effects are calculated and compared with energetic storm particle (ESP) observations. Figure 6 displays a comparison of their theoretical curves with observation for oxygen ions. Similar plots are also available in their paper for C and Fe. Spectral steepening (rollover) effects appear to be reasonably well modeled by their calculations.

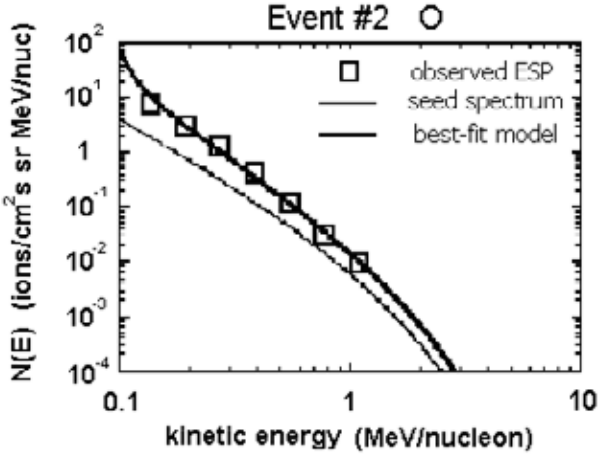

Figure 6. Observed seed spectrum and observed ESP spectrum for oxygen, and best-fit finite-time model for an ACE/ULEIS ESP event

3. SEP propagation

3.1. Background

As compared to the previous ICRC (see Cohen [10]) only a few aspects of the broad topic of solar energetic particle (SEP) propagation have been addressed. The basic scenario is unchanged: SEPs injected at the Sun (with various possible temporal, spatial, and energy scales) propagate through spatially and temporally varying magnetic fields to observers to 1 AU or beyond. The shock moves outward through the solar wind and continues to accelerate SEPs at progressively lower energies. Shocks can affect both propagation and acceleration of SEPs. The basic goal in this field is to understand how seed particles are selected and accelerated by shocks (or by other processes), and to describe the temporal and spatial distribution of the acceleration and propagation of the SEPs.

3.2 Injections and Onsets

From the viewpoint of understanding the acceleration at the flare site it is crucial to determine the time when the first particles are released from the Sun (SEP injection and onset of acceleration). The arrival times are determined by various factors like the time profile of the injection, as well as the scattering, convection, and adiabatic cooling of particles along the path to the observation point. Saiz *et al.* [11] pointed out that the widely used method dubbed "onset time vs. 1/β", based on the assumption that the first arriving particles propagate scatter-free and parallel to the average magnetic field, is an oversimplification, and leads to incorrect results.

The usual initial assumption is that for an observer at 1 AU the length of the Parker spiral is D (for an average solar wind speed of 400 km/s D is about 1.2 AU, but it changes from event to event), so the time of arrival of SEP at speed v is $t_{onset} = t_{inj} + D/v$ where t_{inj} is the time of injection. Under such an assumption, fitting a straight line to t_{onset} vs. $c/v = 1/\beta$ for particles with different velocities, should yield both the injection time t_{inj} and D for the SEP population. Saiz *et al.* argued that sophisticated numerical models using reasonable injection and propagation parameters for protons over a wide range of energy (2 to 2000 MeV) result in onset times which are often incorrect by up to 10 minutes, as indicated in the fits of Figure 7. The propagation distance D is really significantly longer (~1.5 AU, but sometimes even twice longer than naively expected) because the pitch angles of these particles are not zero. It is pointed out that the goodness of t_{onset} vs. $1/\beta$ fits alone does not justify a simple linear relationship.

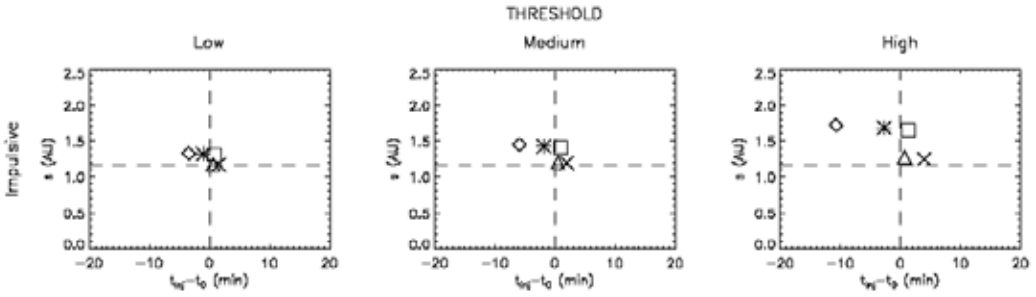

Figure 7. Times of injection vs. path lengths estimated from the inverse velocity fits for impulsive injection. Different symbols denote different mean free path assumptions. Intersections of dashed lines indicate actual values of injection times and path lengths in the simulations. The three panels correspond to increasing thresholds of detection relative to the peak fluxes.

3.3 Decay Phases

Whereas most of both experimental analysis and theoretical work related to SEP events concentrate on the temporal intensity profiles up to the maximum, recent work indicates that the decay phases bear important additional information. Kecskeméty *et al.* [12] extended their earlier statistical analysis, which indicated the general dominance of exponential decay of SEP proton fluxes in the majority of events over a time period extending over two solar cycles. The time constant related with the decay is consistent with the prediction by Lee [13] assuming adiabatic deceleration of SEPs but neglecting diffusion: $\tau = 3R(2 + \alpha\ \gamma)/2V$ (R radial distance, V solar wind speed). The comparison of simultaneous observations aboard Helios, IMP, and Ulysses suggested that τ indeed increases with R but less than linearly. A simulation including scattering with radial diffusion coefficient κ_{rr} increasing with R reproduced the radial variation of τ and indicated that

diffusion indeed is not negligible. The basic problem of determining the decay constant in SEP events is that they are often interrupted by subsequent SEP events or by shock passages that modify decay profiles. This necessitates new observations in the inner heliosphere (< 0.5 AU) where the decays are faster and therefore less frequently affected by subsequent events. The proposed NASA Sentinels mission of 4 spacecraft would be the first inner heliospheric mission since Helios I and II (~1974-85). The Sentinels launch could occur in 2015, whereas the Solar Orbiter of ESA is also expected to visit the inner heliosphere around 2013.

Struminsky *et al.* [14] suggested that two modes of decay are possible during SEP events. For the first, SEPs propagate along magnetic field lines with large azimuthal (cross-field) gradients present. The second mode corresponds to the idea of a particle reservoir, first proposed by McKibben *et al.* [15], with spatial gradients absent, having slow temporal intensity decays with constant energy spectra (invariant spectra), as illustrated in Figure 8. It is important that the reservoir effect appears to extend to high latitudes (Ulysses) as well as to large longitudinal distances in the ecliptic plane. This cannot be the result of a CME bottle containing the "reservoir" as previously thought, because CMEs are about 1 steradian in angular size.

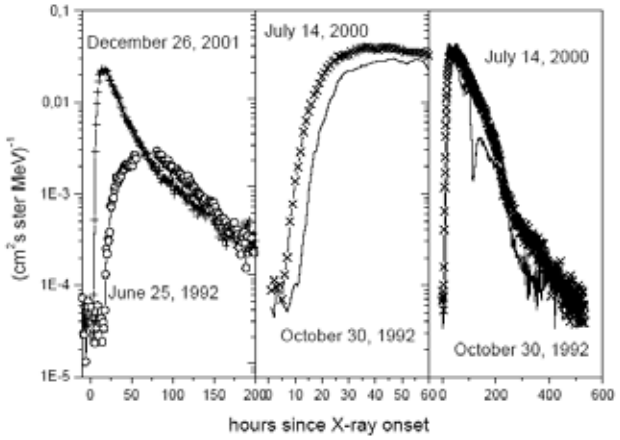

Figure 8. Comparison of 38-125 MeV proton fluxes observed by Ulysses KET at high-latitude polar [December 26, 2001 (2.5 AU, N67) and July 14, 2000 (3.2 AU, S62)] and low-latitude distant [June 25, 1992 (5.3 AU, S12) and October 30, 1992 (5.17 AU, S19)] locations during those events. The middle panel is an expanded scale of the right panel.

SEPs can be used as tracers of the large-scale structure and topology of the interplanetary magnetic field. Malandraki *et al.* [16] discussed two interplanetary CMEs during the October-November 2003 events and found closed looped field structures connected to the Sun at both ends. Le [17] compared the October 28, 2003 SEP event with the Bastille-day event, and suggested that the variation of SEP fluxes as recorded at the geostationary orbit do not properly reflect the true SEP flux variation in the interplanetary space below 30 MeV.

4. Radiation environment at Mars

The new NASA Vision for Space Exploration (VSE) has focused attention on the radiation environment of Mars for manned exploration. In particular, the need to characterize and predict the galactic cosmic ray (GCR) and SEP environment to the orbit of Mars at 1.5 AU has emerged. GCRs provide most of the radiation affecting astronauts, but SEPs can produce highly variable fluxes and accumulate significant doses over short time periods. At Mars SEPs become less important, but GCRs more important than at Earth; also particles accelerated by corotating shocks become more important at > 1 AU.

Adams *et al.* [18] discussed the following requirements for manned missions: to be able to predict worst-case GCR intensities; to work out models for SEP event prediction; and to provide real-time prediction of SEP profiles at SEP event onsets. Astronauts are exposed to most of the radiation dose during the cruise phase since they spend less time on Mars.

4.1 SEP events

Contemporaneous multispacecraft observations at different radial distances and longitudes are helpful to disentangle temporal variations from spatial structures. Miyasaka *et al.* [19] compared nearly 3 years of SEP observations aboard the Japanese spacecraft Nozomi with those at ACE in the period of 1999-2002. During this period Nozomi spent most of its time at about 1.3 AU, and about half as many SEP events were detected on Nozomi as on ACE, although the data coverage of the Nozomi Electron and Ion Spectrometer was only about 60%. Of the 117 ACE and 55 Nozomi SEP events 23 were observed in common. The longitudinal extents of both proton and electron SEP events were probed. The 29 March 2000 fast backside halo CME produced a SEP event on Nozomi, but not on ACE.

4.2 GCR modeling

Mewaldt *et al.* [20] in section SH3.5 of this ICRC used a cosmic-ray transport model based on solar-minimum and maximum GCR spectra to evaluate the radiation dose and dose-equivalent of GCRs. Their preliminary findings indicate that the solar-minimum dose-equivalent is somewhat lower than estimated earlier, with smaller differences between minimum and maximum. In another work, the radiation doses on MARIE/Mars Odyssey were reproduced to within 10% with Earth-based neutron monitor data using an 85-day time lag and the NASA model HZETRN code (Saganti et al. [21]).

Acknowledgements

J. Kóta is thanked for his advice and contributions to this rapporteur talk. The International Space Science Institute (Bern) is acknowledged for supporting the Hungarian co-authors in a related project.

References

1] D. Ruffolo, Ap. J., 442, 861 (1995)
C.K. Ng, D.V. Reames, and A.J Tylka, Ap. J., 591, 461 (2003)
A.J. Tylka, J. Geophys. Res., 106, 25333 (2001)
[2] M.A. Lee, Rev. Geophys. Space Phys. 21, 324-338 (1983)
[3] J.M. Ryan, Rapporteur paper, Proc. 29th ICRC, Pune, 10, 357 (2005).
[4] C.M.S. Cohen et al., Proc. 29th ICRC, Pune, 1, 311 (2005).
[5] V.E. Timofeev and A.T. Filippov, Proc. 29th ICRC, Pune, 1, 289 (2005).
[6] C.M.S. Cohen et al., Proc. 29th ICRC, Pune, 1, 327 (2005).
[7] E.G. Berezhko and S.N. Taneev, Proc. 29th ICRC, Pune, 1, 323 (2005).
[8] C. Channok et al., Paper submitted for the 29th ICRC, Pune, (2005), ID code: tha-channok-C-abs1-sh22.
[9] B.E. Gordon et al., J. Geophys. Res. 104, 28263 (1999).
[10] C.M.S. Cohen, Proc. 28th ICRC, Tsukuba, Frontiers in Cosmic Ray Science 43, 8, 113 (2005).
[11] A. Saiz et al., Proc. 29th ICRC, Pune, 1, 297 (2005).
[12] K. Kecskeméty et al., Proc. 29th ICRC, Pune, 1, 343 (2005).
[13] M.A. Lee, AIP Conf. Proc. 528, 3 (2000).

[14] A.B. Struminsky, Proc. 29th ICRC, Pune, 1, 285 (2005).
[15] B. McKibben et al., J. Geophys. Res. 77, 3957 (1972)
[16] O.E. Malandraki et al., Proc. 29th ICRC, Pune, 1, 269 (2005).
[17] G.M. Le, Paper submitted for the 29th ICRC, Pune, (2005), ID code: chn-le-GM-abs1-sh21.
[18] J.H. Adams et al., Proc. 29th ICRC, Pune, 1, 301 (2005).
[19] H. Miyasaka et al., Proc. 29th ICRC, Pune, 1, 315 (2005).
[20] R.A. Mewaldt et al., Proc. 29th ICRC, Pune, 2, 433 (2005).
[21] P. Saganti et al., Proc. 29th ICRC, Pune, 1, 319 (2005).